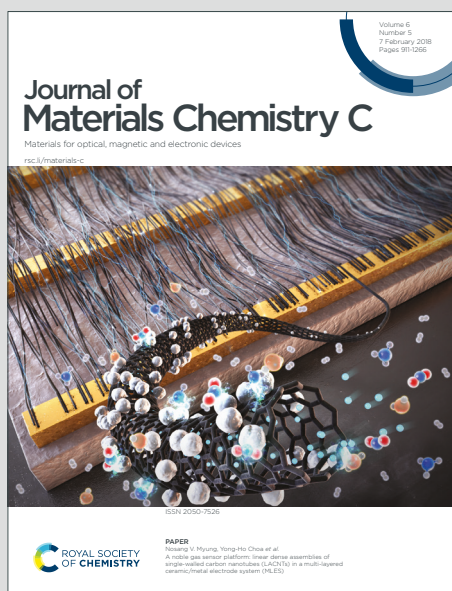


Journal of Materials Chemistry C

Materials for optical, magnetic and electronic devices

Accepted Manuscript

This article can be cited before page numbers have been issued, to do this please use: D. Karthik, D. H. Ahn, J. H. Ryu, H. Lee, J. H. Maeng, J. Y. Lee and J. H. Kwon, *J. Mater. Chem. C*, 2020, DOI: 10.1039/C9TC05950D.



This is an Accepted Manuscript, which has been through the Royal Society of Chemistry peer review process and has been accepted for publication.

Accepted Manuscripts are published online shortly after acceptance, before technical editing, formatting and proof reading. Using this free service, authors can make their results available to the community, in citable form, before we publish the edited article. We will replace this Accepted Manuscript with the edited and formatted Advance Article as soon as it is available.

You can find more information about Accepted Manuscripts in the [Information for Authors](#).

Please note that technical editing may introduce minor changes to the text and/or graphics, which may alter content. The journal's standard [Terms & Conditions](#) and the [Ethical guidelines](#) still apply. In no event shall the Royal Society of Chemistry be held responsible for any errors or omissions in this Accepted Manuscript or any consequences arising from the use of any information it contains.

ARTICLE

Highly Efficient Blue Thermally Activated Delayed Fluorescence Organic Light Emitting Diodes Based on Tercarbazole Donor and Boron Acceptor Dyads

Received 00th January 20xx,
Accepted 00th January 20xx

DOI: 10.1039/x0xx00000x

Durai Karthik, Dae Hyun Ahn, Jae Hong Ryu, Hyuna Lee, Jee Hyun Maeng, Ju Young Lee* and Jang Hyuk Kwon*

Two new blue TADF emitters, namely, 9'-(2,12-di-*tert*-butyl-5,9-dioxa-13b-boranaphtho[3,2,1-*de*]anthracen-7-yl)-9,9''-diphenyl-9*H*,9'*H*,9''*H*-3,3':6',3''-tercarbazole (**3CzTB**) and 9'-(5,9-dioxa-13b-boranaphtho[3,2,1-*de*]anthracen-7-yl)-6,6''-dimethyl-9,9''-diphenyl-9*H*,9'*H*,9''*H*-3,3':6',3''-tercarbazole (**M3CzB**) for application in highly efficient organic light-emitting diode are reported. These emitters consist of tercarbazole as donor and rigid oxygen bridged boron as acceptor units. Despite having the same donor and acceptor segments, an alkyl modification on the periphery of donor and acceptor units altered their physicochemical properties and electrochemical stability of the emitters. Blue TADF light-emitting devices fabricated with these emitters exhibited maximum external quantum efficiency (EQE) and luminance of 30.7%, 18,160 cd/m² and 29.1%, 11,690 cd/m² for **M3CzB** and **3CzTB**, respectively. An operational lifetime (LT₅₀) of stable blue TADF device fabricated with these emitters exhibited 81 hrs and 60.5 hrs at 400 nits with maximum EQE and CIE color coordinates of 14.4%, (0.13, 0.19) and 7.6%, (0.14, 0.10) for **M3CzB** and **3CzTB**, respectively.

Introduction

Organic light-emitting diodes (OLEDs) have emerged as the potential light source in lighting and display technologies over conventional light sources due to their low power consumption, high brightness, less weight, large viewing angle and low cost.^{1,2} Although OLEDs have commercialized in solid-state and flexible displays, their efficiency and operational lifetime are still a bottleneck challenge in display technology. In practical, the usage of blue emitters are still behind green and red emitters in terms of efficiency.³ Though high-efficiency blue phosphorescence (PH) emitters are available, they suffer from high cost, color purity and device operating lifetime.⁴⁻⁶ Alternatively, blue TADF materials have developed with superior efficiency and color purity.⁷⁻⁹ However, TADF emitters also suffer from operating lifetime.^{10,11} Hence, the development of potential TADF emitters satisfying both high efficiency and device lifetime is highly desirable. In general, efficient TADF materials should have small singlet (S₁) and triplet (T₁) energy gap (ΔE_{ST}) for facile reverse intersystem crossing (RISC) process.¹² An effective strategy to reduce the ΔE_{ST} is reducing the overlap between highest occupied molecular orbital (HOMO) and lowest unoccupied molecular orbital (LUMO).

However, highly efficient TADF material cannot only be developed with low ΔE_{ST} , it also requires high photoluminescence quantum yield (PLQY) and high horizontal dipole orientation.^{13,14} A rigid/planar conjugated molecular skeleton can bring both high PLQY and horizontal dipole orientation.¹⁵ Importantly, donor and acceptor interaction maintaining high S₁ and T₁ energy required for blue emission is also an essential consideration. Along with the above prerequisites, the TADF material should be thermally and electrochemically stable in order to achieve durability of the device. Thus, the design of efficient blue TADF emitter is challenging and requires a deep understanding of structure-property relations. Therefore, the development of highly efficient blue TADF material requires careful selection of donor and acceptor segments.

Among the available several donors, carbazole and its derivatives are promising candidates for blue OLED materials due to their high triplet energy, high PLQY and rigid delocalized electronic structure.¹⁶ Among the carbazole-based donors, tercarbazole donor is interesting as it offers high horizontal orientation and high PLQY due to the long rod-like extended conjugation. It was demonstrated that the tercarbazole donor-based material exhibited higher efficiency than mono and bicarbazole donor-based materials due to higher horizontal dipole orientation factor (0.95) of tercarbazole than mono (0.66) and bicarbazole (0.89) donor-based materials.¹⁷ Later, it was also demonstrated that the tercarbazole-based TADF emitter showed higher efficiency and longer device lifetime than indolocarbazole and bicarbazole donor-based TADF emitters due to the low ΔE_{ST} and short delayed exciton lifetime of the former.¹⁸ Though tercarbazole-based materials showed

Organic Optoelectronic Device Laboratory, Department of Information Display, Kyung Hee University, Seoul 02447, Republic of Korea. E-mail: jhkwon@khu.ac.kr, juyoung105@khu.ac.kr.

Electronic Supplementary Information (ESI) available: A detailed synthetic experimental procedure, solvatochromism, time resolved photoluminescence spectra. TGA and DSC graphs, device diagram, ¹H and ¹³C NMR spectra of new materials. See DOI: 10.1039/x0xx00000x

superior performances than other carbazole donor-based materials, their device efficiency and durability together are not satisfactory. Generally, the prevention of active 3,6-positions of carbazole-based donor materials showed enhanced lifetime due to the electrochemical stability of the materials by inhibiting electrochemical polymerization reaction.¹⁹⁻²¹ So, the prevention of such active positions of tercarbazole donor could enhance the durability of the device. On the other hand, boron-based acceptors are promising for high efficiency TADF devices.²² Recently, our group reported highly efficient deep blue TADF emitters based on symmetrical oxygen bridged boron acceptor.²³ The high efficiency originated from the planar extended conjugation of boron acceptor which led to horizontal dipole orientation factor of 0.89. Another advantage of boron acceptor is that it has relatively weak acceptor nature than triazine and sulfone-based acceptors which helps to control the donor-acceptor interaction so as to maintain the high singlet energy (S_1) suitable for blue emission.

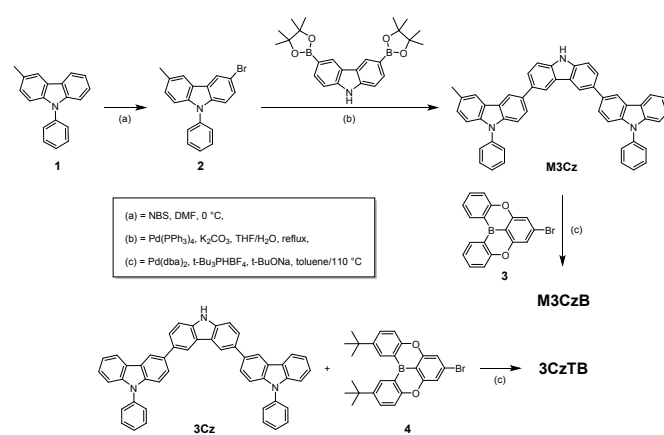
In this work, we report two new blue TADF emitters 9'-(2,12-di-*tert*-butyl-5,9-dioxa-13b-boranaphtho[3,2,1-*de*]anthracen-7-yl)-9,9''-diphenyl-9*H*,9'*H*,9''*H*-3,3':6',3''-tercarbazole (**3CzTB**) and 9'-(5,9-dioxa-13b-boranaphtho[3,2,1-*de*]anthracen-7-yl)-6,6''-dimethyl-9,9''-diphenyl-9*H*,9'*H*,9''*H*-3,3':6',3''-tercarbazole (**M3CzB**) based on tercarbazole donor linked with boron acceptor. The structure of the materials is shown in Fig. 1a. An incorporation of methyl group at active positions of tercarbazole increased the electrochemical stability of **M3CzB**. On the other hand, incorporation of *tert*-butyl group on the boron acceptor decreased the donor-acceptor interaction leading to high ΔE_{ST} of **3CzTB**. The blue TADF device fabricated with these emitters showed maximum external quantum efficiency (EQE) of 30.7% and 29.1% for **M3CzB** and **3CzTB**, respectively. Also, a stable blue TADF device with **M3CzB** exhibited operating lifetime (LT_{50}) of 81 hrs with maximum EQE of 14.4% and CIE coordinates of (0.13, 0.19) at 400 nits. To the best of our knowledge, this is the best result of tercarbazole-based blue TADF device satisfying both efficiency and lifetime together reported so far.

Results and discussion

Molecular design and synthesis

As described in the introduction section tercarbazole donor and symmetrical oxygen bridged boron acceptor has been selected to design highly efficient blue TADF emitters. In order to increase the electrochemical stability of the emitter, the methyl group incorporation at the active 6,6'-positions of tercarbazole donor would be ideal to prevent the electrochemical polymerization reaction under applied voltage. So, we introduced a new 6,6'-dimethyl substituted tercarbazole (**M3Cz**) donor as shown in Scheme 1. Also, to determine the relative electrochemical stability of **M3Cz**-donor, methyl group modified tercarbazole (**3Cz**) donor was also compared. On the other hand, the *tert*-butyl modified boron acceptors (**4** – with *tert*-butyl and **3** – without *tert*-butyl) have been selected to attach with the tercarbazole-based donor segment. It is

believed that the alkyl modification of acceptor would tune the acceptor strength resulting in change in the donor-acceptor interaction. Thus, we envisaged that an alkyl modification on the donor/acceptor moieties could influence the material stability, physicochemical and electroluminescence properties. The synthetic scheme of the new emitters is shown in Scheme 1. The starting materials **3Cz** and **4** were synthesized according to the reported procedures^{15, 23} and the new acceptor **3** was synthesized as the similar procedure used for **4** using phenol as starting material instead of 4-(*tert*-butyl)phenol. The new donor **M3Cz** was synthesized in two steps starting from 3-methyl-9-phenyl-9*H*-carbazole (**1**). Finally, the target materials were synthesized by palladium catalyzed Buchwald-Hartwig cross coupling amination reaction between the corresponding donor and acceptor. The structure of the newly synthesized materials were characterized by ¹H and ¹³C NMR and high resolution mass spectrometry (HRMS).



Scheme 1. Synthetic route of the emitters **M3CzTB** and **3CzTB**.

Theoretical investigation

Density functional theory (DFT) calculation was performed to optimize the ground state geometry and time dependent DFT (TDDFT) was performed to analyze the electronic properties of **3CzTB** and **M3CzB** using B3LYP method with 6-311g basis set on Gaussian 16. The dihedral angle between the donor and acceptor is 52.09° and 51.48° for **3CzTB** and **M3CzB**, respectively. The HOMO is located on the tercarbazole donor with small contribution on the acceptor segment. The LUMO is localized on the entire acceptor moiety and on the nitrogen atom of central carbazole group as shown in Fig. 1b. The well separated HOMO and LUMO orbitals would give small ΔE_{ST} . The calculated ΔE_{ST} is 0.10 eV for both materials. The small ΔE_{ST} of these materials would expect to give good TADF performances. The oscillator strength of these materials was also calculated to be 0.2161 and 0.1888 for **3CzTB** and **M3CzB**, respectively. The difference in their oscillator strength may originate from their different electronic nature which is tuned by the alkyl groups.

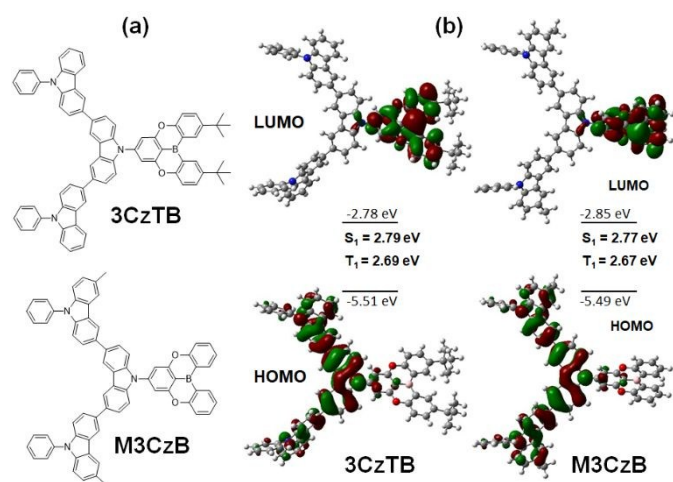


Fig. 1. (a) Molecular structures of new materials. (b) Molecular orbitals and their energy levels.

Photophysical properties

The absorption and photoluminescence properties of these materials were evaluated in dilute toluene solutions. The related spectra of these materials are shown in Fig. 2 and the data are listed in Table 1. The lower wavelength absorption originates from the tercarbazole delocalized π - π^* transition and the higher wavelength absorption attributed to the intramolecular charge transfer (ICT) from the tercarbazole donor to boron acceptor. The material M3CzB exhibited blue-shifted and lower ICT absorption peak than 3CzTB suggests lower ICT interaction of the former in the ground state. Both materials showed deep blue emission in solution. In contrary to the absorption spectra, M3CzB exhibited red-shifted photoluminescence (PL) than 3CzTB suggests more donor-acceptor interaction in the excited state of the former material. This behaviour is due to the absence of *tert*-butyl group in acceptor segment of M3CzB increased the acceptor strength resulting in higher ICT interaction. To confirm this ICT interaction in the excited state PL solvatochromism of these materials were measured and shown in Fig. S1. The degree of red-shift extension from non-polar hexanes (HX) to polar methylenechloride (MC) is more in case of M3CzB that is 113 nm shift, whereas 3CzTB showed 104 nm shift. This result indicates that the better donor-acceptor interaction of M3CzB would show better TADF behaviour than 3CzTB. The low temperature PL (LTPL) spectra were measured to evaluate the T_1 energy of these materials. Both materials showed similar LTPL spectra with vibronically fine profile suggests the triplet state originated from the triplet local excited state (3LE). Further, to confirm the origination of the triplet state, LTPL spectra of both corresponding donors and acceptors were recorded in toluene solution and shown in Fig. S2. This result shows the triplet origination of dopants are dominated by their donor segments rather than their acceptors. The singlet and triplet energies of these materials were obtained from the onset of room temperature PL (RTPL) and LTPL spectra, respectively. The calculated ΔE_{ST} values of 3CzTB and M3CzB are

0.23 eV and 0.14 eV, respectively. These values are adequate in order to have efficient reverse intersystem crossing (RISC) process. Despite having similar triplet energies, the smaller ΔE_{ST} of M3CzB is due to strong ICT character which decreased the S_1 energy. Further, these results indicate that the incorporation of methyl group on the donor segment have negligible influence on the triplet states, whereas incorporation of *tert*-butyl groups on the acceptor part have significant influence on the ICT character which greatly alters the ΔE_{ST} of the materials.

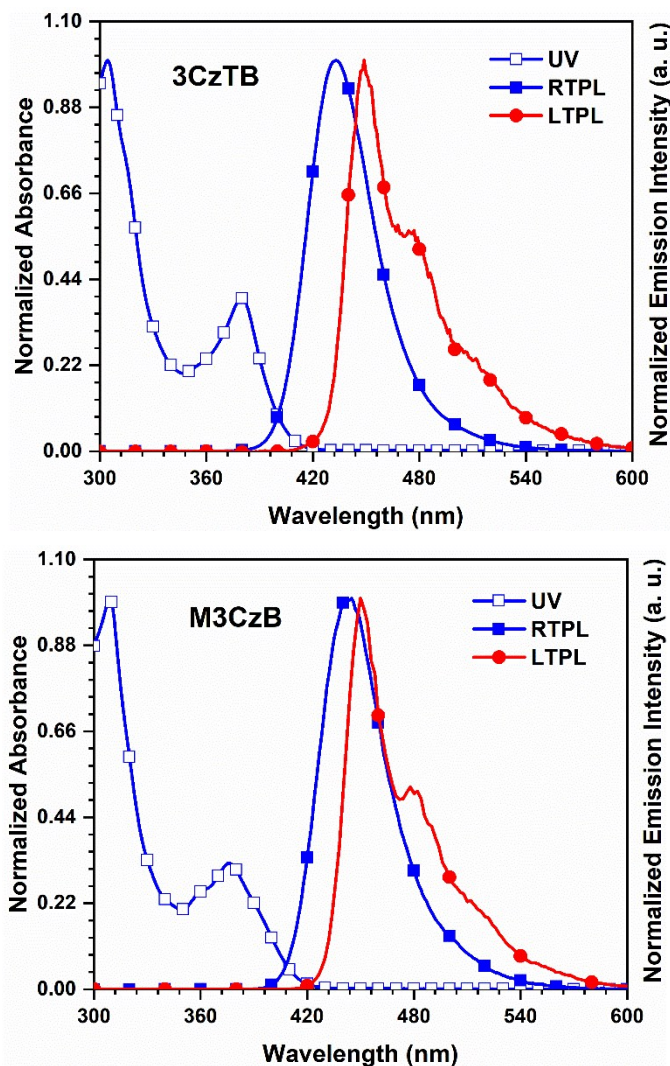


Fig. 2. Absorption and photoluminescence spectra of materials recorded in toluene.

The temperature dependant time resolved photoluminescence decay of the emitters were recorded for the 20 wt% doped in DBFPO films and shown in Fig. 3. The delayed portion increases on increasing the temperature for both materials indicates the existence of TADF properties. Both materials showed bi-exponential decay corresponding to prompt and delayed emission. The prompt and delayed lifetimes of the emitters 3CzTB and M3CzB are 23.40 ns, 9.32 μ s and 88.20 ns, 7.84 μ s, respectively. The M3CzB showed little higher delayed portion and lower delayed lifetime than 3CzTB due to low ΔE_{ST} of the

former. This indicates the **M3CzB** possess facile RISC process for the efficient conversion of triplet to singlet excitons. The photoluminescence quantum yield (PLQY) of both materials were also evaluated in 20 wt% doped DBFPO films. The material **M3CzB** showed little higher PLQY than **3CzTB** attributed to higher delayed portion of the former. To know the ease of RISC process different rate constants of the excited state processes were calculated using the reported method²⁴ and listed in **Table S1**. The **M3CzB** showed higher RISC rate (k_{risc}) and lower triplet non-radiative rate (k_{nr}^t) than **3CzTB**. This confirms the involvement of higher delayed portion in **M3CzB** than **3CzTB** is due to the low ΔE_{ST} . Hence, it is expected that the **M3CzB** would show higher TADF performance in its OLED device.

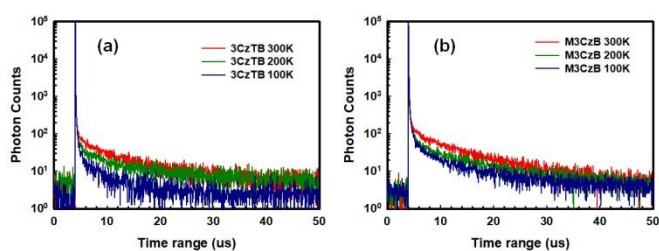


Fig. 3. Temperature dependent time resolved photoluminescence spectra of emitters in 20 wt% doped DBFPO films of (a) **3CzTB** and (b) **M3CzB**.

Electrochemical and thermal properties

To evaluate the redox potentials of the materials cyclic voltammogram was performed using thin film of the materials. The HOMO values were calculated from the oxidation potential of the materials. The calculated HOMO values are -5.63 eV and -5.62 eV for **3CzTB** and **M3CzB**, respectively. The LUMO values were estimated from the HOMO and band gap values. The band gap values were obtained from their absorption onset. The slightly lower band gap of **M3CzB** (2.95 eV) than **3CzTB** (2.99 eV) suggests the enhanced donor-acceptor interaction of the former. The calculated LUMO values are -2.64 eV and -2.67 eV for **3CzTB** and **M3CzB**, respectively. The methyl group in the **M3CzB** increased the HOMO level by 0.01 eV and *tert*-butyl group in **3CzTB** increased the LUMO level by 0.03 eV. Though both materials possess similar donor and acceptor skeleton, a small change in their band gap and LUMO is due to the *tert*-butyl

group on the acceptor. This result indicates that the methyl groups have negligible influence on the donor strength, whereas the *tert*-butyl groups have small influence on the acceptor strength. The electrochemical stability of these materials were evaluated with five repeated cycles of cyclic voltammogram as shown in **Fig. 4**. The **3CzTB** showed one oxidation on first cycle whereas on second cycle onwards it showed a new lower oxidation peak which is originated from the dimer of the oxidized species formed through oligomerisation reaction *via* the terminal 6,6'-positions of tercarbazole donor. This kind of electrochemical oligomerisation reaction of carbazole is known in the

literature.^{25, 26} On the other hand, the **M3CzB** showed same oxidation peak on all five cycles indicates the prevention of such oligomerisation reaction due to the presence of methyl group at 6,6'-positions of tercarbazole donor. This result suggests the methyl group on the terminal tercarbazole donor increased the electrochemical stability of **M3CzB**. Thermal properties of the materials were evaluated by using thermo gravimetric analysis (TGA) and differential scanning calorimetry (DSC) and shown in **Fig. S3**. The thermal decomposition temperature (T_d) (5% wt loss) of the materials were found to be 513 °C and 527 °C for **3CzTB** and **M3CzB**, respectively. In addition, these materials showed very high glass transition temperature (T_g) of 220 °C and 219 °C for **3CzTB** and **M3CzB**, respectively. These results suggest that these materials possess high thermal stability which is

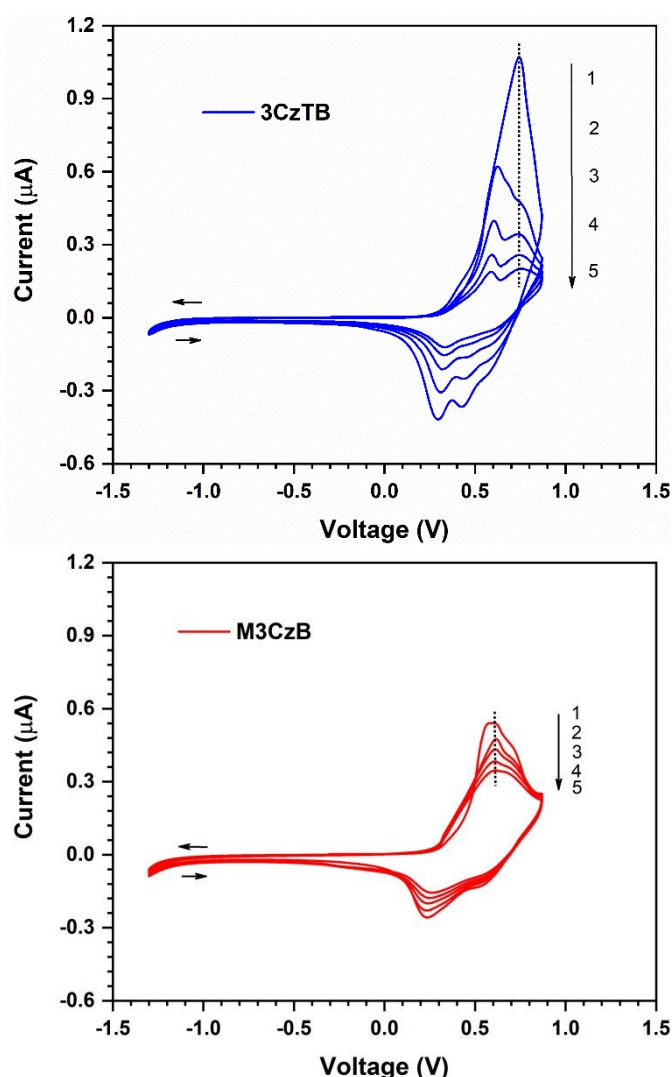


Fig. 4. Cyclic voltammogram of materials measured in thin film up to five repeated cycles.

beneficial for use in stable OLED devices.

Table 1. Photophysical and electrochemical properties of materials.

View Article Online

DOI: 10.1039/C9TC05950D

	$\lambda_{\text{abs}}^{\text{a}}$ (nm)	$\lambda_{\text{em}}^{\text{a}}$ (nm)	S_1^{a} (eV)	T_1^{a} (eV)	ΔE_{ST} (eV) ^a	$\Phi_{\text{p}}^{\text{b}}$ (%)	$\tau_{\text{p}}^{\text{b}}$ (ns)	$\tau_{\text{d}}^{\text{b}}$ (μs)	$k_{\text{risc}} (10^5)^{\text{b}}$ (s^{-1})	HOMO (eV) ^c	LUMO (eV) ^c	Band gap (eV) ^c
3CzTB	380	433	3.16	2.93	0.23	87.8	23.40	9.32	1.02	-5.63	-2.64	2.99
M3CzB	376	445	3.06	2.92	0.14	92.8	88.20	7.84	1.40	-5.62	-2.67	2.95

^a Recorded in toluene solution (10^{-5}M), ^b measured for 20 wt% in DBFPO host, ^c measured for neat film.

Electroluminescence properties

Electroluminescence performance of these materials were evaluated by fabricating blue TADF OLED device with a configuration of ITO (50 nm)/HATCN (7 nm)/TAPC (50 nm)/DCDPA (10 nm)/DBFPO:20 wt% dopant (25 nm)/DBFPO (5 nm)/TPBi (15 nm)/LiF/Al (1.5/100 nm), where ITO (indium tin oxide) used as anode, HATCN (1,4,5,8,9,11-hexaazatriphenylenehexacarbonitrile) used as hole injection layer, TAPC (4,4'-cyclohexylidenebis[*N,N*-bis(4-

methylphenyl)benzenamine]) used as hole transporting layer HTL, DCDPA (3,5-di(9*H*-carbazol-9-yl)-*N,N*diphenylaniline) used as exciton blocking layer (EBL), DBFPO (2,8-bis(diphenylphosphine oxide) dibenzofuran) used as host and EBL and TPBi (1,3,5-tris(1-phenyl-1*H*-benzo[*d*]imidazole-2-yl)benzene) used as electron transporting layer (ETL), LiF/Al used as cathode. The energy level diagram of the structure of the materials used for the fabrication of devices are shown in **Fig. S4**. The electroluminescence performances of these materials are shown in **Fig. 5** and the data are presented in **Table 2**.

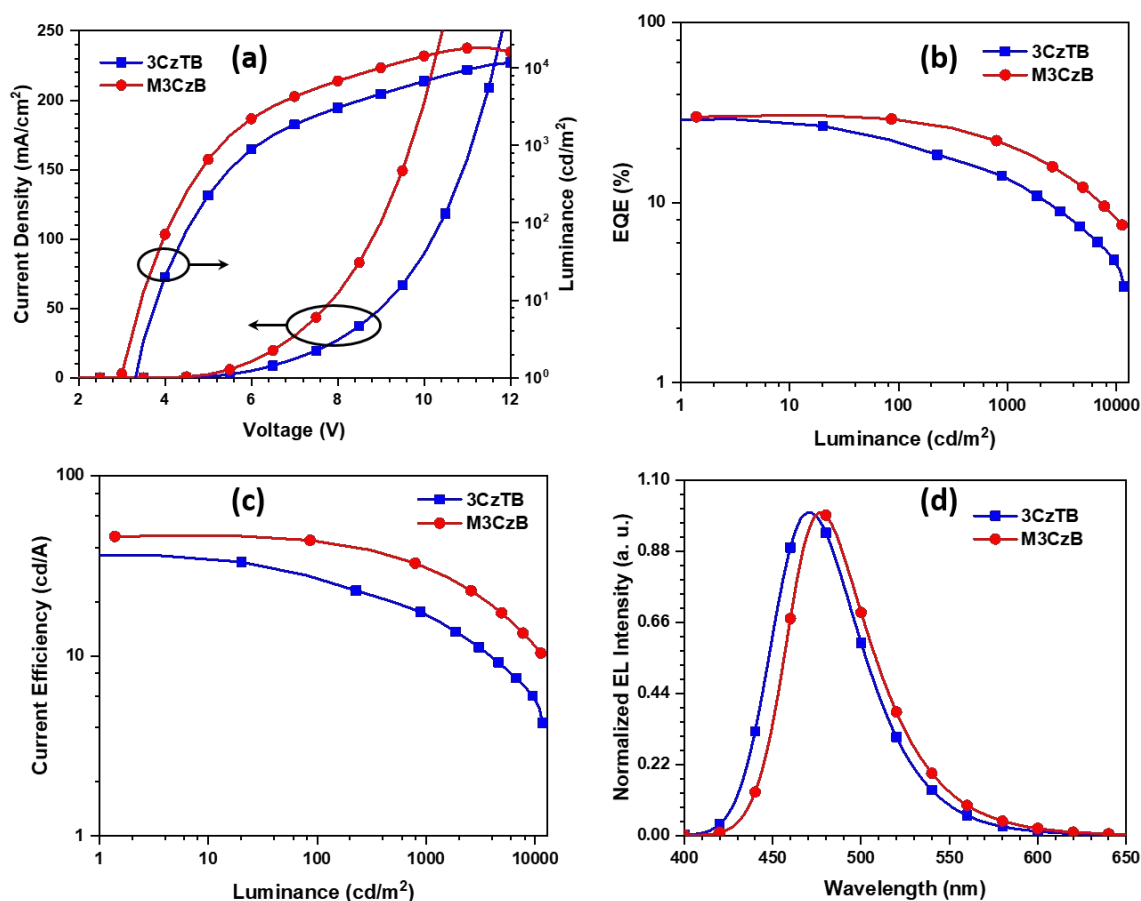


Fig. 5. Electroluminescence properties. (a) J-V-L curve, (b) device efficiency vs luminance, (c) current efficiency vs luminance and (d) electroluminescence spectra.

The current density of **M3CzB**-based device is higher than **3CzTB** indicates the balanced charge collection at the emissive layer in the former device. Although the difference of HOMO and LUMO level is very small between the two emitters, the more bipolar nature of **M3CzB** than **3CzTB** could help charge balance in the

emissive layer in the presence of polar host medium. In addition to that while rationalizing the EL performances using HOMO and LUMO levels charge dipoles formed at the interface of organic layers should also be considered. The existence of charge transfer induced dipoles of the emitter and the charge dipoles formed at the interface of adjacent layers leads to the

shift in the molecular level of organic materials.^{27, 28} So, the difference in current densities and operating voltages observed due to the formation of band offsets. The observed maximum luminance of **M3CzB** and **3CzTB** devices are 18,160 cd/m² and 11,690 cd/m², respectively. The external quantum efficiency (EQE) of these materials were evaluated to be 30.7% and 29.1% for **M3CzB** and **3CzTB**, respectively. The high efficiency of these emitters may attributed to horizontal dipole orientation which is induced by their donor and acceptor molecular skeletons. To confirm this, we have evaluated the horizontal orientation by using TRPL method.²⁹ The experiment was performed for the 20 wt% doped DBFPO films of **3CzTB** and **M3CzB** emitters and compared with the simulation as shown in Fig. 6. As expected, these emitters showed horizontal orientation factor of 0.82 and 0.81 for **3CzTB** and **M3CzB**, respectively. The successful prediction of maximum EQE with the horizontal dipole vs PLQY was demonstrated.^{30,31} Thus, on considering the horizontal

dipole values and the PLQYs of the two emitters, the expected maximum EQE values are almost close with the experimental EQE values. Therefore, this result indicates that the high EQE of these emitters is enhanced by horizontal dipole orientation. The EQE at 1000 cd/m² was 21.6% and 13.5% for **M3CzB** and **3CzTB**, respectively. The efficiency roll-off is severe in case of **3CzTB** (53.6%) when compared to **M3CzB** (29.6%) is due to large ΔE_{ST} and long delayed lifetime. These devices showed high current efficiency of 46.7 cd/A and 36.4 cd/A for **M3CzB** and **3CzTB**, respectively. The EL of these devices showed red-shifted peak than the solution PL spectra due to the polar host medium.³² The CIE color coordinates of these devices are in the blue region of (0.14, 0.19) and (0.14, 0.26) for **M3CzB** and **3CzTB**, respectively. This is the highest efficiency of tercarbazole-based blue TADF OLEDs reported so far with CIEy color coordinates <0.40.

Table 2. Electroluminescence properties of materials.

	V _{on} (v)	Max. luminance (cd/m ²)	CE (cd/A) Max/@1000 cd/m ²	EQE (%) Max/@1000 cd/m ²	EL (nm)	CIE
3CzTB	3.1	11,690	36.4/17.1	29.1/13.5	470	(0.14, 0.19)
M3CzB	3.0	18,160	46.7/31.4	30.7/21.6	478	(0.14, 0.26)

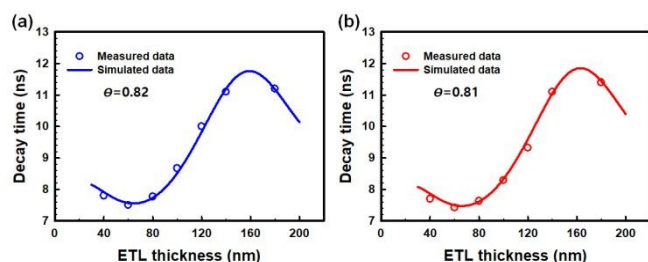


Fig. 6. Measured and simulated radiative decay rate and dipole orientation of 20wt% doped in DBFPO films of (a) **3CzTB** and (b) **M3CzB**.

The device lifetime of the emitters **3CzTB** and **M3CzB** were evaluated by fabricating stable OLED devices. In order to make a stable device some materials were changed as shown in Fig. S5.^{33, 34} The device lifetime (LT₅₀) of these devices were evaluated at 400 nits. The lifetime of devices are 60.5 hrs and 81 hrs for **3CzTB** and **M3CzB**, respectively as shown in Fig. 7. The EQE and CIE of the devices are 7.6% and (0.14, 0.10), 14.4% and (0.13, 0.19) for **3CzTB** and **M3CzB**, respectively. The longer device lifetime of **M3CzB** is attributed to the presence of methyl group on the terminals of the tercarbazole donor and relatively short delayed exciton lifetime. Further, nearly two fold increase of EQE is attributed to low ΔE_{ST} . However, the EQE is lower than the DBFPO hosted devices due to low triplet energy level of mCBP-CN host resulting in some triplet energy loss. It is interesting to compare the lifetime of these devices with the lifetime of TDBA-DI device.²³ The TDBA-DI doped in mCBP-CN host exhibited lifetime (LT₅₀) of 55.2 hrs with EQE and CIE of 21.36% and (0.14, 0.27), respectively, at 1,000 nits. However,

on considering the CIE coordinates, **M3CzB** and **3CzTB** showed deeper blue compared to TDBA-DI. Thus, the **M3CzB** based device is the highly efficient blue TADF device at this color coordinates based on tercarbazole donor-based materials reported so far.¹⁸

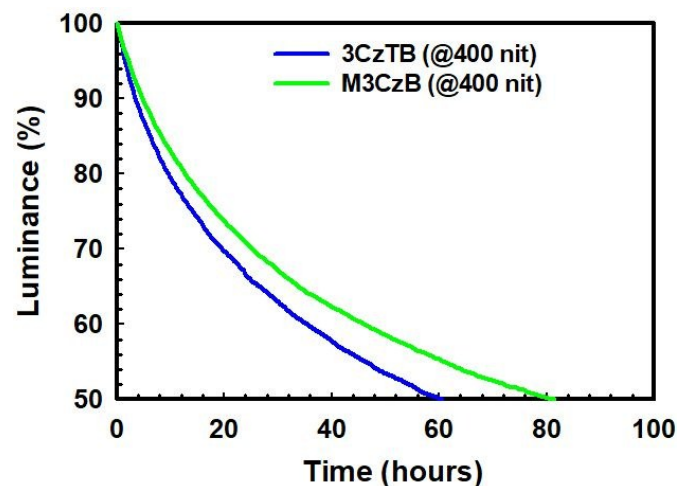


Fig. 7. Electroluminescent device operating lifetime (LT₅₀) at 400 nits.

Conclusion

Two highly efficient blue TADF emitters **M3CzB** and **3CzTB** based on tercarbazole donor and boron acceptor were designed and synthesized to have high PLQY and horizontal dipole orientation. Alkyl modification on the donor and acceptor units tuned their donor-acceptor interaction and electronic nature which altered their photophysical and electrochemical

properties. The absence of *tert*-butyl group on the acceptor of **M3CzB** emitter enhanced the ICT character which was confirmed by lower ΔE_{ST} , higher red-shift in PL solvatochromism and lower bandgap than **3CzTB** emitter. Additionally, the presence of methyl group at 6,6'-positions of tercarbazole donor increased the electrochemical stability of **M3CzB** emitter. The blue TADF OLEDs fabricated with these emitters showed maximum EQE/current efficiency/luminance of 30.7%/46.7 cdA⁻¹/18,160 cdm⁻² and 29.1%/36.4 cdA⁻¹/11,690 cdm⁻² for **M3CzB** and **3CzTB**, respectively. The high efficiency of these devices may attributed to horizontal dipole orientation of these emitters originated from the rigid/planar donor and acceptor skeletons. In addition to that, the stable blue TADF device fabricated with these emitters exhibited device operating lifetime (LT₅₀) of 81 hrs and 60.5% hrs with maximum EQE/CIE coordinates of 14.4%/(0.13, 0.19) and 7.6%/(0.14, 0.10) for **M3CzB** and **3CzTB**, respectively. This result is the best efficient blue TADF device based on tercarbazole TADF emitters reported so far. Thus, we strongly believe that this design tactic would help to design new efficient blue TADF emitters.

Experimental Section

Materials and characterization

All reagents for synthesizing the materials were purchased from Sigma–Aldrich, TCI (SEJINCI) and used as such. 1,4,5,8,9,11-hexaazatriphenylene-hexacarbonitrile (HATCN) was purchased from EM Index. 1,1-bis[(di-4-tolylamino) phenyl] cyclo-hexane (TAPC), and 2,2',2''-(1,3,5-benzinetriyl)-tris(1-phenyl-1-*H*-benzimidazole) (TPBi) were purchased from Jilin OLED Material Tech Co., Ltd. The other materials, 3,5-di(9*H*-carbazol-9-yl)-*N,N*-diphenylaniline (DCDPA), 2,8-bis(diphenylphosphine oxide) dibenzofuran (DBFPO) were synthesized by using the previously reported methods.^{35, 36} For the characterization of photo-physical properties in solution, all materials were prepared in toluene solution at the concentration of 1×10^{-5} M. The UV-vis absorption spectrum was measured by V-750 Spectrophotometer (Jasco). The solution PL spectrum and low temperature (77 K) PL spectrum were measured by FP-8500 Spectrofluorimeter (Jasco). The low temperature PL spectra was measured after 30ms time delay. The absolute PLQY values in doped films were measured by connecting an integrating sphere to the same spectrofluorimeter. These doped films were also used for transient PL measurement. Transient PL was measured when photon counts were reached until 10,000 in a nitrogen environment using Quantaurus-Tau fluorescence lifetime measurement system (C11367-03, Hamamatsu Photonics Co.). Thermal properties of newly synthesized materials were investigated by differential scanning calorimetry (DSC) and thermogravimetric analysis (TGA). The glass transition temperature (T_g) was measured by DSC graph and the decomposition temperatures (T_d) of emitters measured by TGA at 5% weight loss. Electrochemical analyses were performed using EC epsilon electrochemical analysis equipment. To measure the cyclic voltammetry (CV) characteristics of TADF emitters, platinum, carbon wire and Ag wire in 0.01 M AgNO₃,

0.1 M tetrabutyl ammonium perchlorate (Bu₄NClO₄), acetonitrile solution were used as counter, working and reference electrodes, respectively. For supporting electrolyte, 0.1 M tetrabutyl ammonium perchlorate in acetonitrile solution was used. Using an internal ferrocene/ferrocenium (Fc/Fc⁺) standard, the potential values were converted to the saturated calomel electrode (SCE) scale. The optical band-gap was determined from absorption onset. The LUMO level of each material was calculated from both the optical band gap and HOMO level.

Optical simulation

The optical simulations of the OLED devices were performed by using the semiconducting emissive thin film optics simulator (SETFOS 4.3) simulation program, which enabled to input the refractive index (*n*), extinction coefficient (*k*), dipole orientation factor of the emitters, thickness of layers and the emission spectra of emissive layer.

Device fabrication and characterization

To fabricate OLEDs, Indium-Tin-Oxide (ITO) coated glass substrates (50 nm, sheet resistance of 10 Ω/square,) were sequentially cleaned in ultrasonic bath with acetone, and isopropyl alcohol for 10 minutes each, and then rinsed with deionized water. Finally, substrates were dried using nitrogen followed by UV-ozone treatment for 10 minutes. All organic layers and metal cathode were deposited on the pre-cleaned ITO glass by vacuum evaporation technique under a vacuum pressure of $\sim 1 \times 10^{-7}$ torr. The deposition rate of all organic layers in was about 0.5 Å/s. Similarly, the deposition rate of LiF and Al were maintained at 0.1 Å/s, 4.0 Å/s, respectively. Finally, all devices were encapsulated using glass cover and UV curable resin inside the nitrogen filled glove box. The OLED area was 4 mm² for all the samples studied in this work. J-V and L-V characteristics of fabricated OLED devices were measured by using Keithley 2635A SMU and Konica Minolta CS-100A, respectively. EL spectra and CIE 1931 color coordinates were obtained using Konica Minolta CS-2000 spectroradiometer. All measurements were performed in ambient condition.

Conflicts of interest

There are no conflicts to declare.

Acknowledgements

This work was supported by the National Research Foundation of Korea Grant (No. NRF-2019R11A1A01058272) and the Technology Innovation Program (20006464, Development of RGB delayed fluorescent material and ink-jet printing technology with quantum efficiency more than 20% for mass production of large-area OLED) funded By the Ministry of Trade, Industry & Energy (MOTIE, Korea). And this work was also supported by Samsung Display Co., Ltd.

References

- 1 C. W. Tang and S. A. VanSlyke, *Appl. Phys. Lett.*, 1987, **51**, 913-915.
- 2 S. R. Forrest, *Nature*, 2004, **428**, 911-918.
- 3 Y. Im, S. Y. Byun, J. H. Kim, D. R. Lee, C. S. Oh, K. S. Yook and J. Y. Lee, *Adv. Funct. Mater.*, 2017, **27**, 1603007.
- 4 S. Scholz, D. Kondakov, B. Lüssem and K. Leo, *Chem. Rev.*, 2015, **115**, 8449-8503.
- 5 Y. Zhang, J. Lee and S. R. Forrest, *Nat. Commun.*, 2014, **5**, 5008.
- 6 G. Li, K. Klimes, T. Fleetham, Z.-Q. Zhu and J. Li, *Appl. Phys. Lett.*, 2017, **110**, 113301.
- 7 L.-S. Cui, H. Nomura, Y. Geng, J. U. Kim, H. Nakanotani and C. Adachi, *Angew. Chem. Int. Ed.*, 2017, **56**, 1571-1575.
- 8 H. Uoyama, K. Goushi, K. Shizu, H. Nomura and C. Adachi, *Nature*, 2012, **492**, 234.
- 9 Z. Cheng, Z. Li, Y. Xu, J. Liang, C. Lin, J. Wei and Y. Wang, *ACS Appl. Mater. Interfaces*, 2019, **11**, 28096-28105.
- 10 S. K. Jeon, H. L. Lee, K. S. Yook and J. Y. Lee, *Adv. Mater.*, 2019, **31**, 1803524.
- 11 M. Kim, S. K. Jeon, S.-H. Hwang and J. Y. Lee, *Adv. Mater.*, 2015, **27**, 2515-2520.
- 12 Y. Im, M. Kim, Y. J. Cho, J.-A. Seo, K. S. Yook and J. Y. Lee, *Chem. Mater.*, 2017, **29**, 1946-1963.
- 13 X. Zeng, K.-C. Pan, W.-K. Lee, S. Gong, F. Ni, X. Xiao, W. Zeng, Y. Xiang, L. Zhan, Y. Zhang, C.-C. Wu and C. Yang, *J. Mater. Chem. C*, 2019, **7**, 10851-10859.
- 14 K. Shizu, H. Noda, H. Tanaka, M. Taneda, M. Uejima, T. Sato, K. Tanaka, H. Kaji and C. Adachi, *J. Phys. Chem. C*, 2015, **119**, 26283-26289.
- 15 D. Yokoyama, *J. Mater. Chem.*, 2011, **21**, 19187-19202.
- 16 Y. Tao, C. Yang and J. Qin, *Chem. Soc. Rev.*, 2011, **40**, 2943-2970.
- 17 S. Y. Byeon, J. Kim, D. R. Lee, S. H. Han, S. R. Forrest and J. Y. Lee, *Adv. Optical Mater.*, 2018, **6**, 1701340.
- 18 J. G. Yu, S. H. Han, H. L. Lee, W. P. Hong and J. Y. Lee, *J. Mater. Chem. C*, 2019, **7**, 2919-2926.
- 19 D. Zhang, M. Cai, Y. Zhang, D. Zhang and L. Duan, *Mater. Horiz.*, 2016, **3**, 145-151.
- 20 N. Prachumrak, S. Pojanasopa, R. Tarsang, S. Namuangruk, S. Jungsuttiwong, T. Keawin, T. Sudyoadsuk and V. Promarak, *New J. Chem.*, 2014, **38**, 3282-3294.
- 21 T. Fukushima, J. Yamamoto, M. Fukuchi, S. Hirata, H. H. Jung, O. Hirata, Y. Shibano, C. Adachi and H. Kaji, *AIP Adv.*, 2015, **5**, 087124.
- 22 Y. Zhang, D. Zhang, J. Wei, Z. Liu, Y. Lu and L. Duan, *Angew. Chem. Int. Ed.*, 2019, **58**, 16912-16917.
- 23 D. H. Ahn, S. W. Kim, H. Lee, I. J. Ko, D. Karthik, J. Y. Lee and J. H. Kwon, *Nat. Photonics*, 2019, **13**, 540-546.
- 24 K. Masui, H. Nakanotani and C. Adachi, *Org. Electron.*, 2013, **14**, 2721-2726.
- 25 P. Schrögel, A. Tomkevičienė, P. Strohmriegel, S. T. Hoffmann, A. Köhler and C. Lennartz, *J. Mater. Chem.*, 2011, **21**, 2266-2273.
- 26 P. Kotchapradist, N. Prachumrak, R. Tarsang, S. Jungsuttiwong, T. Keawin, T. Sudyoadsuk and V. Promarak, *J. Mater. Chem. C*, 2013, **1**, 4916-4924.
- 27 A. Rajagopal, C. I. Wu and A. Kahn, *J. Appl. Phys.*, 1998, **83**, 2649-2655.
- 28 D. Karthik, K. R. Justin Thomas, J.-H. Jou, S. Kumar, Y.-L. Chen and Y.-C. Jou, *RSC Adv.*, 2015, **5**, 8727-8738.
- 29 I. J. Ko, H. Lee, J. H. Park, G. W. Kim, R. Lampande, R. Pode and J. H. Kwon, *Phys. Chem. Chem. Phys.*, 2019, **21**, 7083-7089.
- 30 S.-Y. Kim, W.-I. Jeong, C. Mayr, Y.-S. Park, K.-H. Kim, J.-H. Lee, C.-K. Moon, W. Brütting and J.-J. Kim, *Adv. Funct. Mater.*, 2013, **23**, 3896-3900.
- 31 K.-H. Kim and J.-J. Kim, *Adv. Mater.*, 2018, **30**, 1705600.
- 32 D. H. Ahn, J. S. Moon, S. W. Kim, S. Y. Lee, D. Karthik, J. Y. Lee and J. H. Kwon, *Org. Electron.*, 2018, **59**, 39-44.
- 33 G. W. Kim, Y. H. Son, H. I. Yang, J. H. Park, I. J. Ko, R. Lampande, J. Sakong, M.-J. Maeng, J.-A. Hong, J. Y. Lee, Y. Park and J. H. Kwon, *Chem. Mater.*, 2017, **29**, 8299-8312.
- 34 S.-G. Ihn, N. Lee, S. O. Jeon, M. Sim, H. Kang, Y. Jung, D. H. Huh, Y. M. Son, S. Y. Lee, M. Numata, H. Miyazaki, R. Gómez-Bombarelli, J. Aguilera-Iparraguirre, T. Hirzel, A. Aspuru-Guzik, S. Kim and S. Lee, *Adv. Sci.*, 2017, **4**, 1600502.
- 35 P. A. Vecchi, A. B. Padmameruma, H. Qiao, L. S. Sapochak and P. E. Burrows, *Org. Lett.*, 2006, **8**, 4211-4214.
- 36 Y. J. Cho and J. Y. Lee, *Adv. Mater.*, 2011, **23**, 4568-4572.

TOC

View Article Online
DOI: 10.1039/C9TC05950D

